Synthesis and Characterization of Borohydride Rare-Earth Complexes Supported by 2-PyridinemethanAmido Ligands and their Application towards Ring-Opening Polymerization of Cyclic Esters

Maxime Beauvois,[a] Frédéric Capet,[a] Joseph W. Ziller,[b] William J. Evans,[b] Yohan Champouret,*[,a] Marc Visseaux*,[a]

[a] Univ. Lille, CNRS, Centrale Lille, Univ. Artois, UMR 8181, UCCS, Unité de Catalyse et Chimie du Solide, F-59000, Lille, France. E-mail : Yohan.champouret@univ-lille.fr, Marc.visseaux@univ-lille.fr.

[b] Department of Chemistry, University of California, Irvine, California 92697-2025, United States

Supplementary Information

Table S1 Crystal data and structure refinement for **PyAH²** and **KN.PyAH¹**		
Compound Name	**PyAH²**	**KN.PyAH¹**
Empirical formula	$C_{20}H_{28}N_2$	$C_{50}H_{88}N_6Si_4K_2$
Formula weight	296.44	963.82
Temperature/K	99.98	93(2)
Crystal system	orthorhombic	triclinic
Space group	$Pca2_1$	P-1
a/Å	14.5286(6)	10.8057(7)
b/Å	11.2578(4)	11.7125(8)
c/Å	22.0519(9)	13.2613(9)
α/°	90	88.7038(10)
β/°	90	71.4150(10)
γ/°	90	64.5690(9)
Volume/Å^3	3606.8(2)	1423.85(17)
Z	8	1
ρ_{calc}g/cm^3	1.092	1.124
μ/mm^{-1}	0.064	0.287
F(000)	1296.0	524.0
Crystal size/mm^3	0.2 × 0.12 × 0.1	0.358 × 0.294 × 0.282
Radiation	MoKα (λ = 0.71073)	MoKα (λ = 0.71073)
2Θ range for data collection/°	3.618 to 56.63	3.886 to 61.08
Index ranges	-19 ≤ h ≤ 19, -14 ≤ k ≤ 15, -29 ≤ l ≤ 29	-15 ≤ h ≤ 15, -16 ≤ k ≤ 16, -18 ≤ l ≤ 18
Reflections collected	70664	36247
Independent reflections	8927 [R_{int} = 0.0641, R_{sigma} = 0.0439]	8597 [R_{int} = 0.0292, R_{sigma} = 0.0233]
Data/restraints/parameters	8927/1/409	8597/0/295
Goodness-of-fit on F^2	1.046	1.068
Final R indexes [I>=2σ (I)]	R_1 = 0.0491, wR_2 = 0.1169	R_1 = 0.0277, wR_2 = 0.0727
Final R indexes [all data]	R_1 = 0.0685, wR_2 = 0.1279	R_1 = 0.0327, wR_2 = 0.0758
Largest diff. peak/hole / e Å^{-3}	0.39/-0.23	0.44/-0.20

Additional structural description for **PyAH²** and KN.**PyAH¹**:

In **PyAH²**, the weak non-bonding H1-$N2_{Pyr}$ interaction could be determined by the fact that the sum of the Van der Waals radii between nitrogen (1.55 Å) and hydrogen (1.20 Å) is larger than the distance found in the XRD data [distance N2(Pyr)-H1 = 2.588(2) Å < $r_N + r_{H =}$ 2.75 Å]. This observation results in a N2-C15-C13-N1 amino-pyridine twist angle of -54.6(3)°, showing a marked deviation of the amino moiety from the pyridine plane. In addition, it is noticed that the aryl ring and the pyridine plane deviate from the orthogonality with an angle of 67.04(9)°.
In KN.**PyAH¹**, The difference in torsion angles of the amino-pyridine moiety between the adduct [N2-C15-C14-N1 = -20.49(10)°] and the free-ligand **PyAH¹** [N2-C15-C14-N1 = 66.4(2)°][18a] shows a structural constraint in the adduct caused by the coordination of the pyridine/amine nitrogens of the protio-ligand to the potassium center. Compared to **PyAH¹**, the deviation from orthogonality between the pyridine and the N-aryl planes is more evident in the adduct [60.58°[18a] in **PyAH¹** *vs.* 45.62(4)° in KN.**PyAH¹**], which might be caused by steric repulsion of the (trimethylsilyl)amide group and the isopropyl substituents of the N-aryl group of **PyAH¹**.

Table S2 Crystal data and structure refinement for **1_Y, 2_Y, $1''_{Nd}$** and **2_{Nd}**				
Compound Name	**1_Y**	**2_Y**	**$1''_{Nd}$**	**2_{Nd}**
Empirical formula	$C_{62}H_{122}B_6MgN_4O_6Y_2$	$C_{38}H_{54}BN_4Y$	$C_{46}H_{74}B_4N_4Nd_2O_2$	$C_{38}H_{54}BN_4Nd$
Formula weight	1286.62	666.57	1046.81	721.90
Temperature/K	99.99	99.93	100.05	100.03
Crystal system	triclinic	monoclinic	monoclinic	monoclinic
Space group	P-1	C2/c	$P2_1/n$	C2/c
a/Å	10.4849(7)	15.8805(4)	9.8551(9)	16.1304(11)
b/Å	10.9594(8)	10.7056(3)	15.2082(14)	10.7594(7)
c/Å	16.5868(12)	22.3241(8)	20.438(2)	22.1049(15)
α/°	85.776(4)	90	90	90
β/°	85.716(4)	107.1020(10)	102.420(4)	107.052(3)
γ/°	70.181(4)	90	90	90
Volume/$Å^3$	1785.7(2)	3627.51(19)	2991.5(5)	3667.7(4)
Z	1	4	2	4
$\rho_{calc}g/cm^3$	1.196	1.221	1.162	1.307
μ/mm^{-1}	1.673	1.638	1.748	1.446
F(000)	690.0	1416.0	1068.0	1500.0
Crystal size/mm^3	0.31 × 0.27 × 0.22	0.23 × 0.16 × 0.14	0.29 × 0.23 × 0.2	0.344 × 0.24 × 0.231
Radiation	MoKα (λ = 0.71073)	MoKα (λ = 0.71073)	MoKα (λ = 0.71073)	MoKα (λ = 0.71073)
2Θ range for data collection/°	2.466 to 55.432	3.818 to 56.508	3.366 to 52.766	3.854 to 61.116
Index ranges	-13 ≤ h ≤ 13, -14 ≤ k ≤ 14, 0 ≤ l ≤	-21 ≤ h ≤ 19, -14 ≤ k ≤ 14, -29 ≤ l	-12 ≤ h ≤ 12, -19 ≤ k ≤ 18, -25 ≤ l	-22 ≤ h ≤ 23, -15 ≤ k ≤ 15, -31 ≤ l

	21	≤ 29	≤ 25	≤ 31
Reflections collected	8210	59875	74200	55659
Independent reflections	8210 [R_{int} = ?, R_{sigma} = 0.0319]	4490 [R_{int} = 0.0404, R_{sigma} = 0.0177]	6095 [R_{int} = 0.0377, R_{sigma} = 0.0262]	5593 [R_{int} = 0.0233, R_{sigma} = 0.0113]
Data/restraints/parameters	8210/456/405	4490/0/227	6095/150/299	5593/0/239
Goodness-of-fit on F^2	1.054	1.045	1.161	1.143
Final R indexes [I>=2σ (I)]	R_1 = 0.0444, wR_2 = 0.1083	R_1 = 0.0230, wR_2 = 0.0572	R_1 = 0.0492, wR_2 = 0.1133	R_1 = 0.0168, wR_2 = 0.0419
Final R indexes [all data]	R_1 = 0.0528, wR_2 = 0.1124	R_1 = 0.0255, wR_2 = 0.0582	R_1 = 0.0642, wR_2 = 0.1221	R_1 = 0.0171, wR_2 = 0.0420
Largest diff. peak/hole / e $Å^{-3}$	1.30/-1.33	0.34/-0.29	1.62/-1.01	0.42/-0.46

Additional structural description for $\mathbf{1_Y}$ and $\mathbf{2_Y}$:

In $\mathbf{1_Y}$, the crystal packing shows, on the same ionic compound, one yttrium bearing the (*R*) ligand and the other one bearing the (*S*) configuration separated by the magnesium cation, as [Y(**PyA**$^{\mathbf{1}}$)$^{(S)}$(BH_4)$_3$][Mg(THF)$_6$][Y(**PyA**$^{\mathbf{1}}$)$^{(R)}$(BH_4)$_3$]. The N-aryl plane deviates from orthogonality with respect to the pyridine ring [68.95(9)°] and is almost identical to that found in the Nd complex (**PyA**$^{\mathbf{2}}$)Nd(BH_4)$_2$(THF)$_2$ ($\mathbf{3'_{Nd}}$), while the amido-pyridine chelate is quasi-planar with a torsion angle of N1-C5-C6-N2 = 14.9(4)°.

In $\mathbf{2_Y}$, the twist angles of the amido-pyridine chelates exhibit notable differences between the coordination of **PyA**$^{\mathbf{1(R)}}$ [N2-C6a-C5-N1 = -12.5(3)°] and **PyA**$^{\mathbf{1(S)}}$ [N2-C6b-C5-N1 = 32.8(3)°] enantiomers to the Y center. The torsion angle of the (*R*) conformer is practically planar and identical to that found in complex $\mathbf{1_Y}$, despite the presence of a second **PyA**$^{\mathbf{1}}$ (*S*) conformer ligand in $\mathbf{2_Y}$ which, conversely, features a structure with a larger twist angle of the amido-pyridine chelate. A comparison of the two (**PyA**$^{\mathbf{1}}$)-yttrium complexes, mono- *vs*. bis-substituted, can be made: while one Y–B length shows a di-hapto coordination mode of one of the borohydride in $\mathbf{1_Y}$, all other BH_4 are in a tri-hapto mode. Both complexes show *quasi*-identical Y-N [Y-N(Pyr) and Y-N(amido), respectively] bond lengths. The observed twist angle of the amido-pyridine chelate in complex $\mathbf{1_Y}$ is quite similar to that obtained when **PyA**$^{\mathbf{1(R)}}$ is coordinated in the bis-substituted complex $\mathbf{2_Y}$, while that seen with **PyA**$^{\mathbf{1(S)}}$ was greater. Already discussed previously, the orthogonality of the pyridine ring to the aryl plane is more pronounced in the bis-substituted complex, probably due to steric hindrance induced by the coordination of the second chelating ligand.

Additional structural description for $\mathbf{1''_{Nd}}$ and $\mathbf{2_{Nd}}$:

In $\mathbf{1''_{Nd}}$, the twist angle of the amido-pyridine chelate [N1-C5-C6-N2 = 3.3(7)°] exhibits a *quasi*-planarity, while the N-aryl ring deviates from orthogonality to the pyridine ring with an angle of 74.9(2)°. The distance between both Nd atoms is found at 4.5726(9) Å.

In $\mathbf{2_{Nd}}$, the torsion angle of the amido-pyridine chelate is not the same depending on the (*R*) or (*S*) enantiomers. While the chelate of the (*S*) configuration is slightly out of planarity [N1-C5-C6a-N2 = 11.0(3)°], the chelate of the (*R*) configuration is highly distorted according to the twist angle N1-C5-C6b-N2 = -31.2(4)°, which is similar to what was described for $\mathbf{2_Y}$. As such, the coordination of the **PyA**$^{\mathbf{1(R)}}$ on the neodymium results in the same torsion angle than the coordination of **PyA**$^{\mathbf{1(S)}}$ on the yttrium and *vice versa* [N-C-C-$N_{Nd(PyA1R)2}$ ≈ N-C-C-N $_{Y(PyA1S)2}$ ≠ N-C-C-$N_{Nd(PyA1S)2}$ ≈ N-C-C-N $_{Y(PyA1R)2}$]. The N-aryl group slightly deviates from orthogonality with respect to the pyridine ring by a few degrees [angle between the two planes: 85.58(5)°]. Finally, complex $\mathbf{2_{Nd}}$ has a τ of 0.46,[1] very similar

to the value found for $\mathbf{2_Y}$, which implies the same kind of distortion between square pyramidal and trigonal bipyramidal geometries, probably caused by the borohydride group.

Table S3 Crystal data and structure refinement for $\mathbf{3'_{Nd}}$, $\mathbf{4_{Nd}}$ and $\mathbf{5_Y}$			
Compound Name	$\mathbf{3'_{Nd}}$	$\mathbf{5_Y}$	$\mathbf{4_{Nd}}$
Empirical formula	$C_{28}H_{51}B_2N_2NdO_2$	$C_{50}H_{86}B_2LiN_3O_4Y$	$C_{34}H_{54}B_2N_3Nd$
Formula weight	613.56	910.68	670.66
Temperature/K	100.13	108	100.14
Crystal system	monoclinic	monoclinic	monoclinic
Space group	$P2_1/c$	C2/c	$P2_1/c$
a/Å	11.5979(3)	16.2361(7)	13.2907(4)
b/Å	19.9655(4)	20.0771(8)	16.2120(5)
c/Å	13.3459(3)	32.0329(16)	17.2538(5)
α/°	90	90	90
β/°	91.3750(10)	101.858(2)	110.7420(10)
γ/°	90	90	90
Volume/Å^3	3089.46(12)	10219.1(8)	3476.69(18)
Z	4	8	4
ρ_{calc}g/cm^3	1.319	1.184	1.281
μ/mm^{-1}	1.705	1.185	1.518
F(000)	1276.0	3928.0	1396.0
Crystal size/mm^3	0.24 × 0.19 × 0.16	0.29 x 0.24 x 0.12	0.25 × 0.11 × 0.09
Radiation	MoKα (λ = 0.71073)	MoKα (λ = 0.71073)	MoKα (λ = 0.71073)
2Θ range for data collection/°	3.512 to 66.244	3.268 to 56.53	3.562 to 56.54
Index ranges	-15 ≤ h ≤ 17, -30 ≤ k ≤ 30, -20 ≤ l ≤ 20	-21 ≤ h ≤ 21, -26 ≤ k ≤ 26, -42 ≤ l ≤ 42	-17 ≤ h ≤ 17, -21 ≤ k ≤ 21, -22 ≤ l ≤ 22
Reflections collected	135932	167324	109657
Independent reflections	11753 [R_{int} = 0.0349, R_{sigma} = 0.0183]	12650 [R_{int} = 0.0533, R_{sigma} = 0.0228]	8595 [R_{int} = 0.0594, R_{sigma} = 0.0252]
Data/restraints/parameters	11753/0/358	12650/0/593	8595/46/424
Goodness-of-fit on F^2	1.069	1.036	1.058
Final R indexes [I>=2σ (I)]	R_1 = 0.0174, wR_2 = 0.0474	R_1 = 0.0355, wR_2 = 0.0850	R_1 = 0.0338, wR_2 = 0.0967
Final R indexes [all data]	R_1 = 0.0221, wR_2 = 0.0481	R_1 = 0.0447 wR_2 = 0.0893	R_1 = 0.0405, wR_2 = 0.0992
Largest diff. peak/hole / e Å^{-3}	0.48/-0.53	0.53/-0.68	1.39/-0.95

Additional structural description for **3'$_{Nd}$**, **5$_{Y}$** and **4$_{Nd}$**:

Packing of complex **3'$_{Nd}$** exhibits both ligands coordinated to the Nd center with (*R*) and (*S*) enantiomers in the unit cell. The twist angle of the 2-pyridinemethanamido chelate in **3'$_{Nd}$** [N1-C5-C7-N2 = 18.90(14)°] is found between the two values observed in **2$_{Nd}$** for the (*R*) and (*S*) configuration of the coordinated **PyA^{1}** ligand [N1-C5-C6a-N2 = 11.0(3)° and N1-C5-C6b-N2 = 31.2(4)°]. Moreover, the N-aryl group deviates more from orthogonality with the pyridine plane in **3'$_{Nd}$** [69.19(4)°], compared to **2$_{Nd}$** [85.58(5)°]. However, this deviation is almost identical to that found in (**PyA^{1}**)-substituted yttrium complex [(**PyA^{1}**)Y(BH_4)$_3$]$_2$(Mg(THF)$_6$ (**1$_{Y}$**) (*vide supra*).

In **5$_{Y}$**, the ene-amido-pyridine (N1-C13-C15-N2) and amido-pyridine (N3-C20-C19-N2) chelates deviate slightly from orthogonality, with torsion angles of 5.9(2)° and 16.3(2)°, respectively. Furthermore, the N(amino)-aryl plane is practically perpendicular to the pyridine ring [88.5(2)°], unlike the N(ene-amido)-aryl planes, which have an angle of 70.5(2)° with the pyridine.

In **4$_{Nd}$**, the torsion angles between the imino-pyridine chelating moiety [N3-C13-C15-N1 = -1.3(4)°] shows that it is more planar, due to conjugation between the imine group and the pyridine ring, than the amido-pyridine chelate [N1-C19-C20-N2 = -24.1(3)°]. The difference between N(imine)-aryl and N(amido)-aryl groups also influences the orientation of their respective planes in relation to the pyridine ring. Specifically, the angle formed by the pyridine ring and the N(imine)-aryl plane is 80.53(12)°, indicating a lesser degree of orthogonality compared to the N(amido)-aryl plane one, which formed an angle of 91.22(9)° with the former.

Table S4 Crystal data and structure refinement for (**PyA^2**)- and (**PyA^3**)-Mg complexes		
Compound Name	(**PyA^2**)Mg(BH_4)(THF)	(**PyA^3**)Mg(BH_4)(THF)
Empirical formula	$C_{24}H_{39}BMgN_2O$	$C_{38}H_{58}BMgN_3O$
Formula weight	406.69	607.99
Temperature/K	100.06	100.05
Crystal system	monoclinic	monoclinic
Space group	$P2_1/c$	$P2_1/c$
a/Å	11.6575(4)	10.0564(8)
b/Å	18.0090(6)	16.3418(12)
c/Å	12.3915(3)	22.4870(17)
α/°	90	90
β/°	99.6880(10)	102.785(2)
γ/°	90	90
Volume/Å^3	2564.37(14)	3603.9(5)
Z	4	4
ρ_{calc}g/cm^3	1.053	1.121
μ/mm^{-1}	0.085	0.082
F(000)	888.0	1328.0
Crystal size/mm^3	0.35 × 0.31 × 0.28	0.19 × 0.11 × 0.11
Radiation	MoKα (λ = 0.71073)	MoKα (λ = 0.71073)
2Θ range for data collection/°	3.544 to 60.97	3.108 to 51.332
Index ranges	-16 ≤ h ≤ 16, -25 ≤ k ≤ 25, -17 ≤ l ≤ 16	-12 ≤ h ≤ 12, -19 ≤ k ≤ 19, -27 ≤ l ≤ 27
Reflections collected	95391	75277
Independent reflections	7802 [R_{int} = 0.0515, R_{sigma} = 0.0284]	6820 [R_{int} = 0.0469, R_{sigma} = 0.0313]
Data/restraints/parameters	7802/0/284	6820/0/424
Goodness-of-fit on F^2	1.110	1.047
Final R indexes [I>=2σ (I)]	R_1 = 0.0361, wR_2 = 0.1017	R_1 = 0.0497, wR_2 = 0.1169
Final R indexes [all data]	R_1 = 0.0477, wR_2 = 0.1053	R_1 = 0.0698, wR_2 = 0.1266
Largest diff. peak/hole / e Å^{-3}	0.34/-0.20	1.17/-0.44

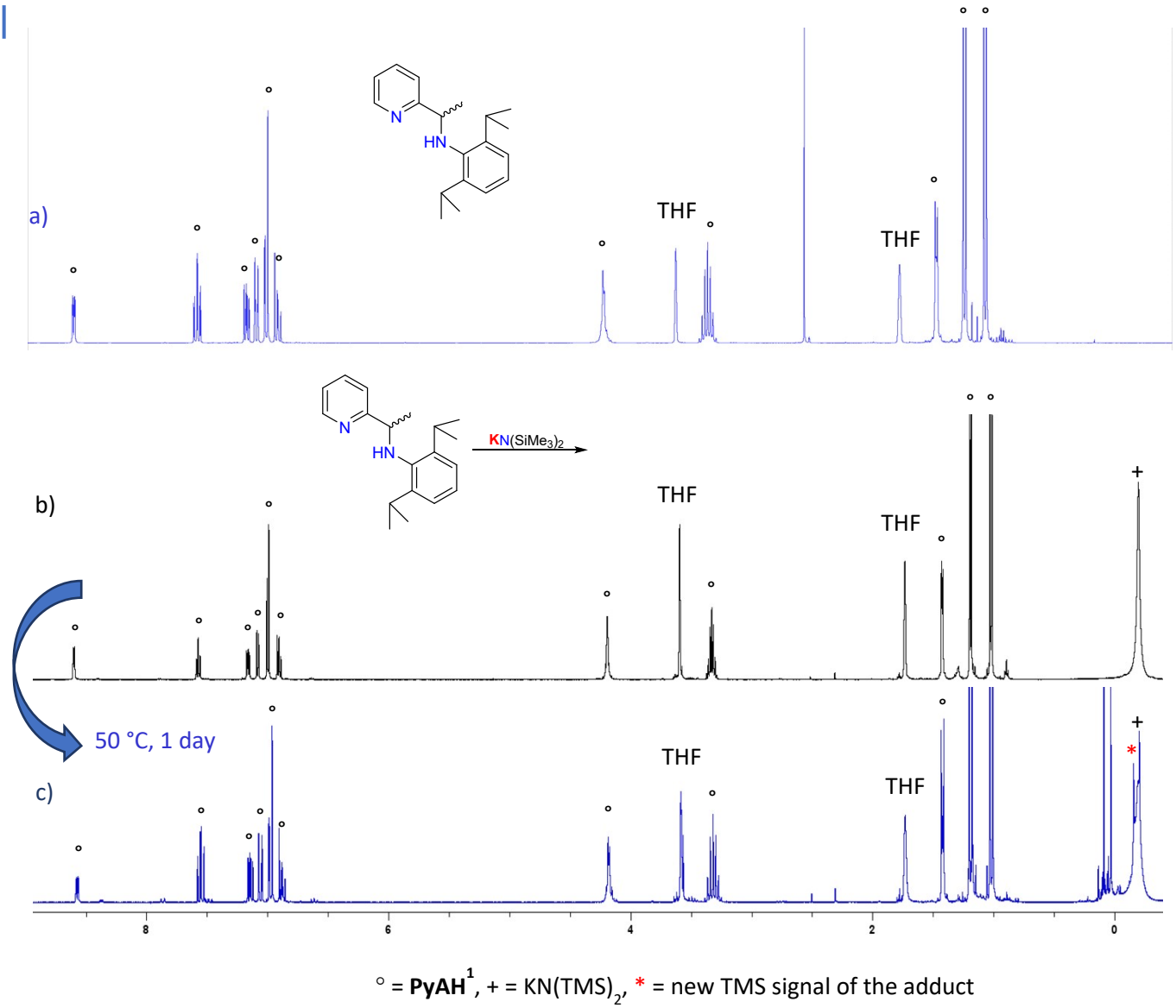

° = **PyAH**[1], + = $KN(TMS)_2$, * = new TMS signal of the adduct

Fig. S1 ^1H NMR spectrum (THF-D_8) of **PyAH**[1] (a, top), immediately after addition of $KN(SiMe_3)_2$ (b, middle, with (o) and (+) revealing the signals of **PyAH**[1] and $KN(SiMe_3)_2$, respectively) and after heating at 50 °C for 7 days (b, bottom), showing no difference for **PyAH**[1] resonances (the signals labelled (*) are attributed to partial hydrolysis ($(HN(SiMe_3)_2$).

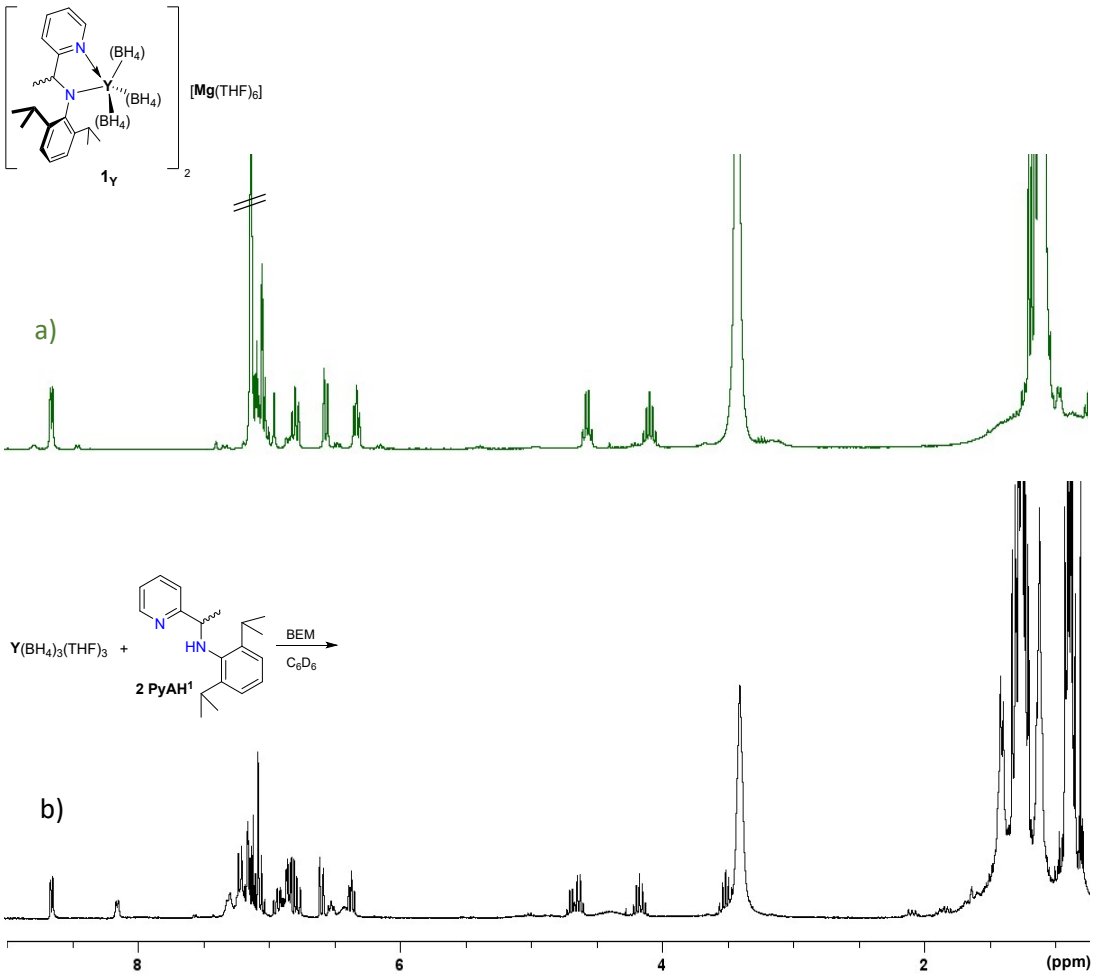

Fig. S2 ^{1}H NMR spectrum (C_6D_6) of isolated complex **1**$_{Y}$ from bulk synthesis (a, green) and of the mixture [$Y(BH_4)_3(THF)_3$ + 2 **PyAH^{1}** + 1 BEM] obtained at the NMR scale (b, black).

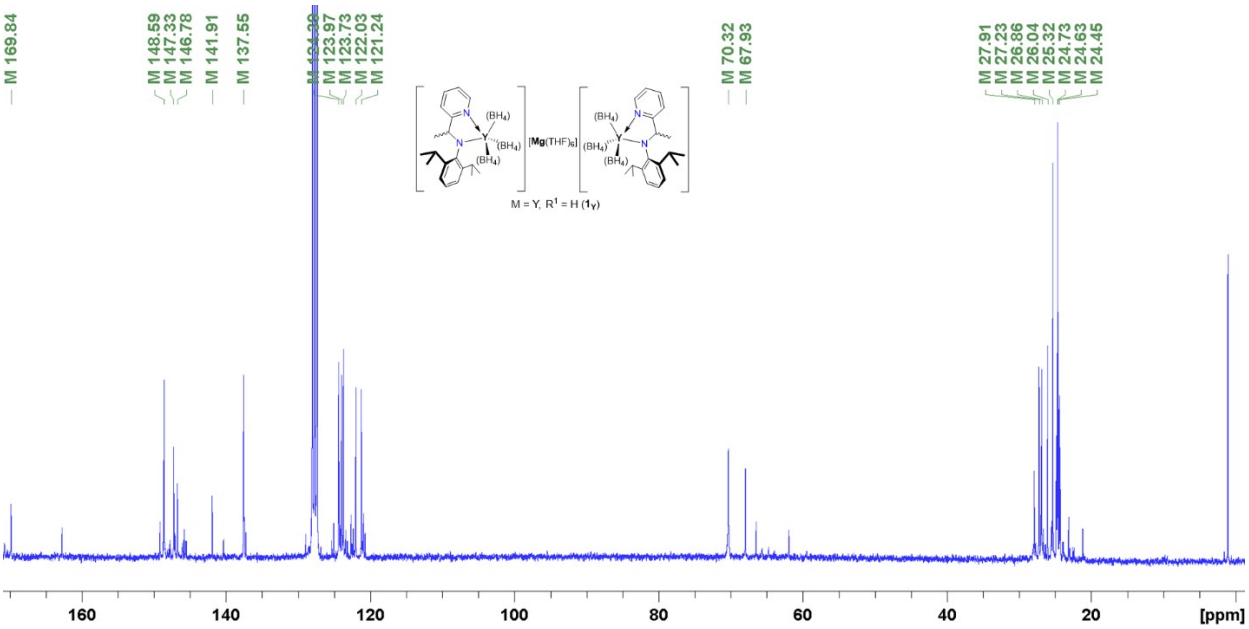

Fig. S3 ^{13}C NMR spectrum of $\mathbf{1_Y}$ (C_6D_6)

It is worth noting that the coordination of the **PyA^1** ligand to yttrium borohydride disrupts the symmetry plane, allowing the distinction of each carbon in the isopropyl groups as well as the carbons in the aryl group. Therefore, for complex **[(PyA^1)Y(BH$_4$)$_3$]$^-_2$[Mg(THF)$_6$]$^{2+}$($\mathbf{1_Y}$)**, a total of 19 carbon signals are anticipated from the coordinated **PyA^1** ligand, in addition to 2 signals from the THF molecules. The ^{13}C NMR spectrum (75 MHz, C_6D_6, Fig. S3) shows chemical shifts (δ, ppm) at 24.45, 24.63, 24.73, 25.32, 26.04, 26.86, 27.23, 27.91 for ($\underline{C}H_3)_2\underline{C}H$-, THF and -N-C(H)($\underline{C}H_3$)- (8 signals); 70.32, 67.93 for THF and -N-$\underline{C}$(H)(CH_3)- (2 signals); and 121.24, 122.03, 123.73, 123.97, 124.38, 137.55, 141.91, 146.78, 147.33, 148.59, 169.84 for the pyridine and aryl groups (11 signals).

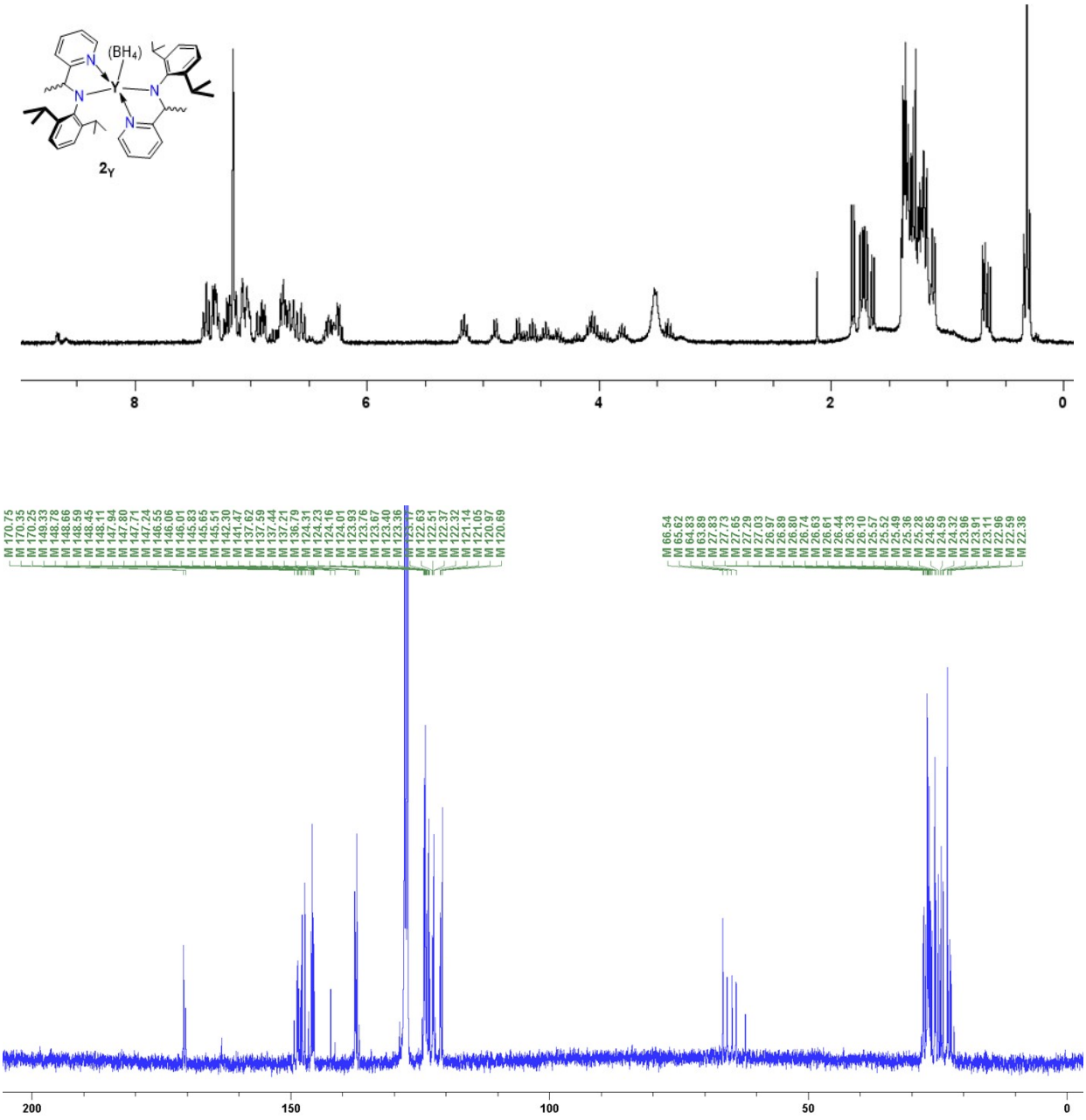

Fig. S4 a) ^{1}H NMR (top) and b) ^{13}C NMR (bottom) spectra of the crystals of complex $\mathbf{2_Y}$

The disruption of the symmetry plane in complex **$(PyA^1)_2Y(BH_4)$ (2_Y)** (as seen in complex $\mathbf{1_Y}$), along with the presence of two ligands per Y metal, leads to multiplication of carbons signals. We observed 4 sets of signals for 4 stereoisomers and a total of 76 carbon signals in the ^{13}C NMR spectrum (75 MHz, C_6D_6, Fig. S4) at δ (ppm) = 22.38, 22.59, 22.96, 23.11, 23.91, 23.96, 24.32, 24.59, 24.85, 25.28, 25.36, 25.49, 25.52, 25.57, 26.10, 26.33, 26.44, 26.61, 26.63, 26.74, 26.80, 26.89, 26.97, 27.03, 27.29, 27.65, 27.73, 27.83 for ($\underline{C}H_3)_2\underline{C}H$- and -N-C(H)($\underline{C}H_3$)- (28 signals); 63.89, 64.83, 65.62, 66.54 for -N-$\underline{C}$(H)(CH_3)- (4 signals); and 120.69, 120.97, 121.05, 121.14, 122.32, 122.51, 122.63, 123.17, 123.36, 123.40, 123.67, 123.76, 123.93, 124.01, 124.16, 124.23, 124.31, 136.79, 137.21, 137.44, 137.59, 137.62, 141.47, 142.30, 145.51, 145.83, 146.01, 146.06, 146.55, 147.24, 147.71, 147.80, 147.94, 148.11, 148.45, 148.59, 148.66, 148.78, 149.33, 170.25, 170.35, 170.75 for the pyridine and aryl groups (42 signals).

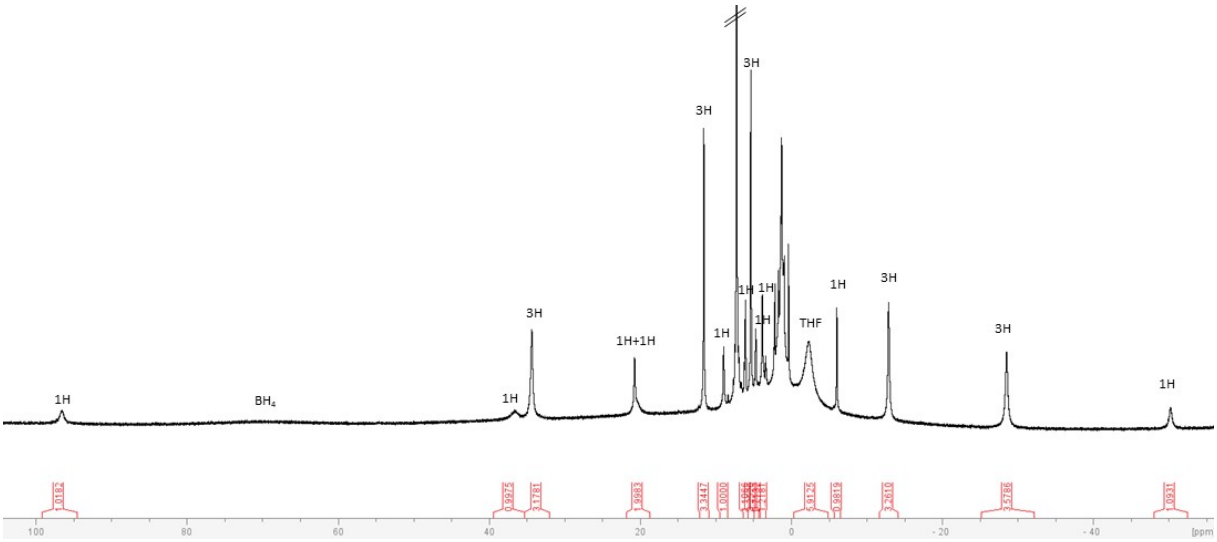

Fig. S5 ^{1}H NMR spectrum of **1'$_{Nd}$** (C_6D_6)

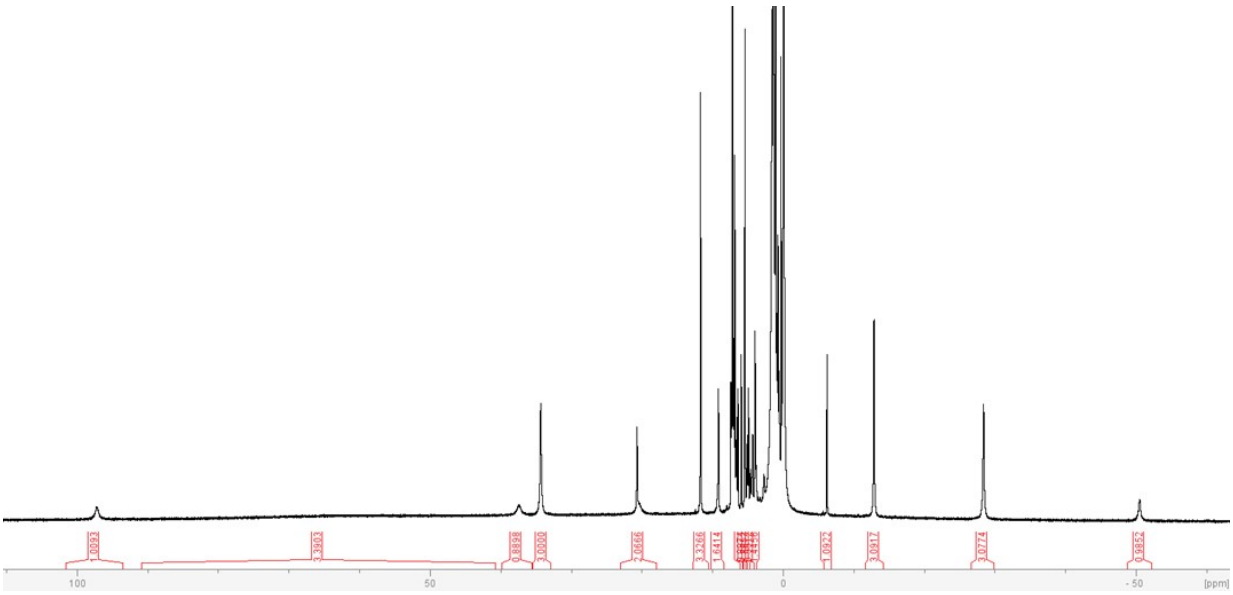

Fig. S6 ^{1}H NMR (C_6D_6) spectrum of complex $\mathbf{1_{Nd}}$, which is also similar to that obtained from the reaction $(C_3H_5)Nd(BH_4)_2(THF)_3$ + **PyAH**[1]

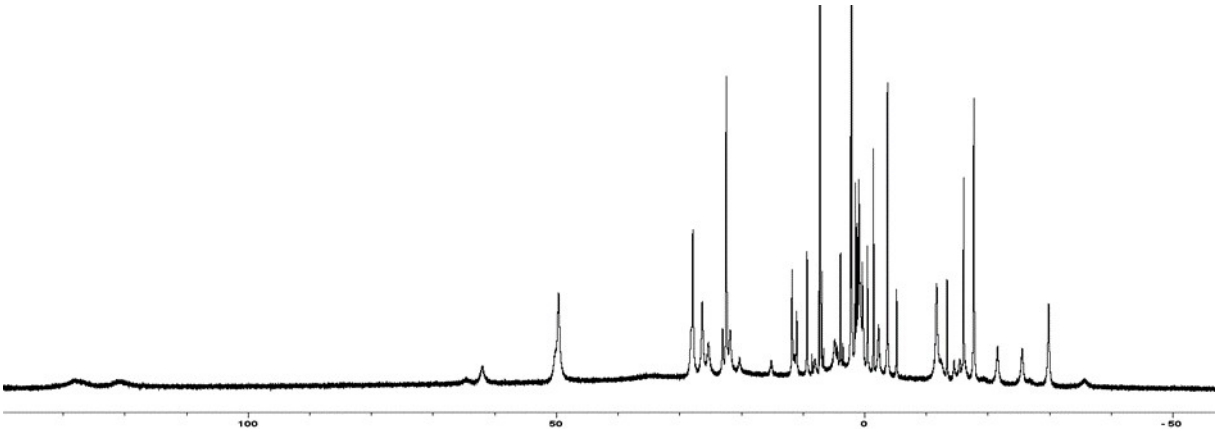

Fig. S7 ^{1}H NMR of isolated crystals of complex $\underline{\mathbf{2}}_{\mathbf{Nd}}$ (C_6D_6)

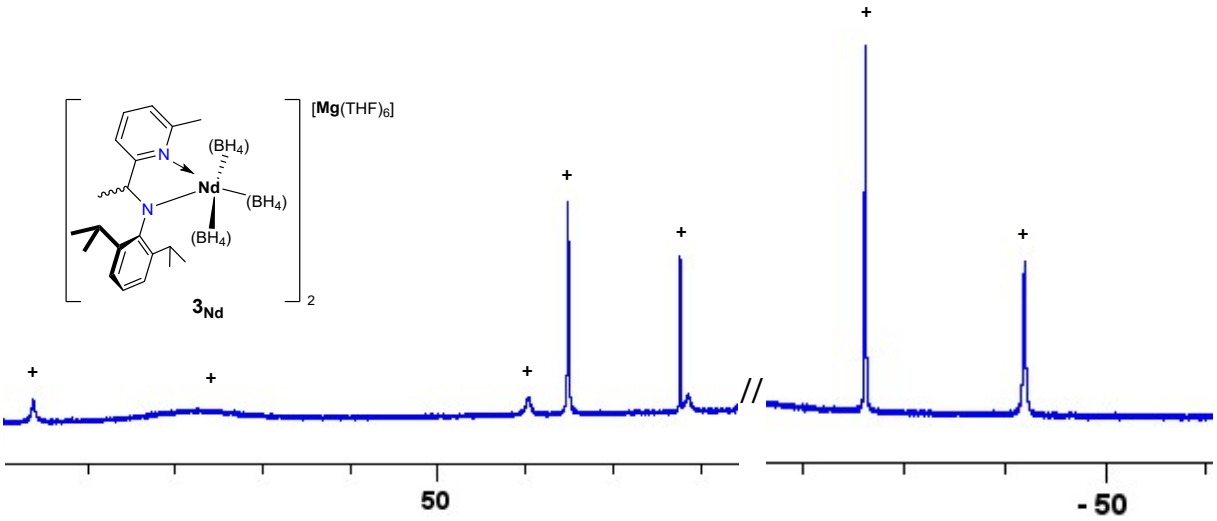

Fig. S8 ^{1}H NMR (paramagnetic zone) of complex $\mathbf{3_{Nd}}$ in C_6D_6

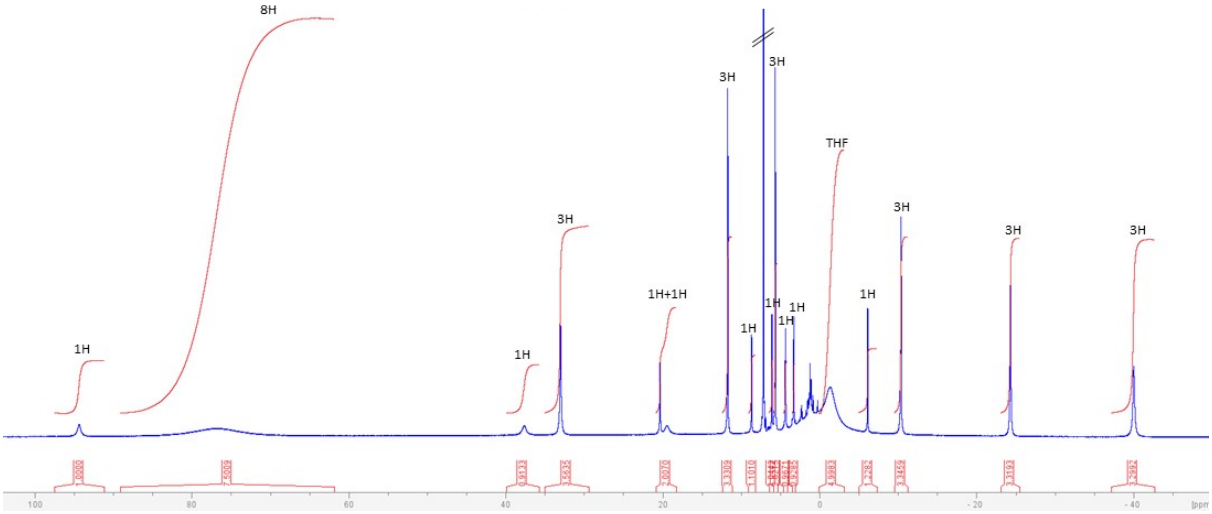

Fig. S9 ^{1}H NMR spectrum of **3'$_{Nd}$** (C_6D_6).

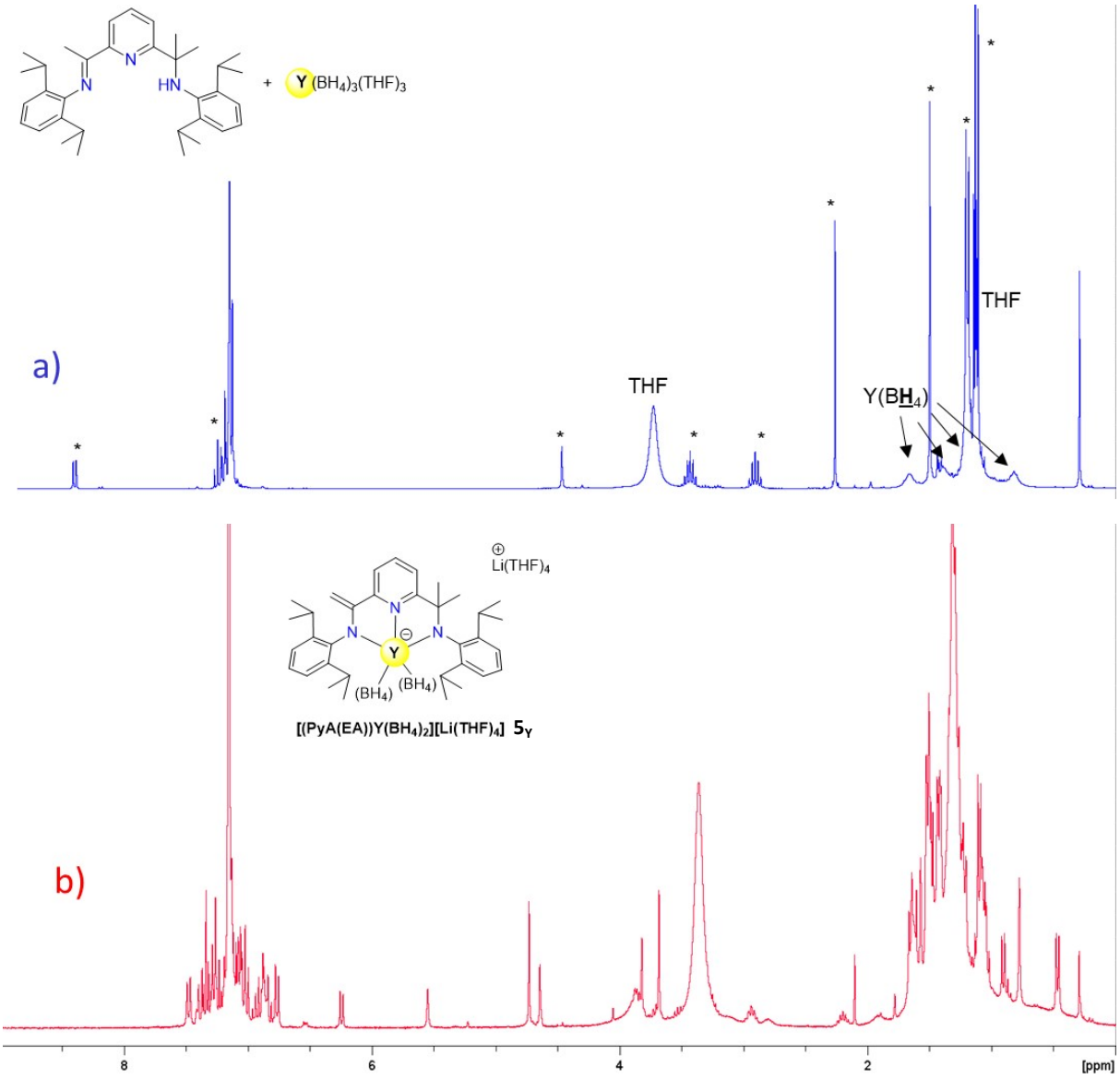

Fig. S10 ^{1}H NMR spectrum of the mixture $Y(BH_4)_3(THF)_3$ and 1 equiv. of **PyAH³** (a, top, blue, * **PyAH³**) and of the isolated complex [(**PyA(EA)**)$Y(BH_4)_2$][$Li(THF)_4$] (**5$_Y$**) (b, bottom, red) (solvent C_6D_6)

The ^{1}H NMR spectra of **5$_Y$** were recorded in C_6D_6 (Fig S10b) and THF-D_8 (Fig S11b) and compared with the mixture of $Y(BH_4)_3(THF)_3$ and **PyAH³** before deprotonation (Figs. S10a and S11a). The spectra could not be properly interpreted, but we could clearly identify a shift of the proton resonances of the ligand relative to **5$_Y$** in both NMR solvents. In C_6D_6, proton signals between δ = 5.5 and 6.5 ppm were observed, which could correspond to the protons of the ene-amido group. In addition, a shift of the proton signals of the BH_4 groups, around 0 ppm for $Y(BH_4)_3(THF)_3$ in THF-D_8, could be detected in [(**PyA(EA)**)$Y(BH_4)_2$][$Li(THF)_4$] (**5$_Y$**), thus corroborating that a complexation reaction has taken place.

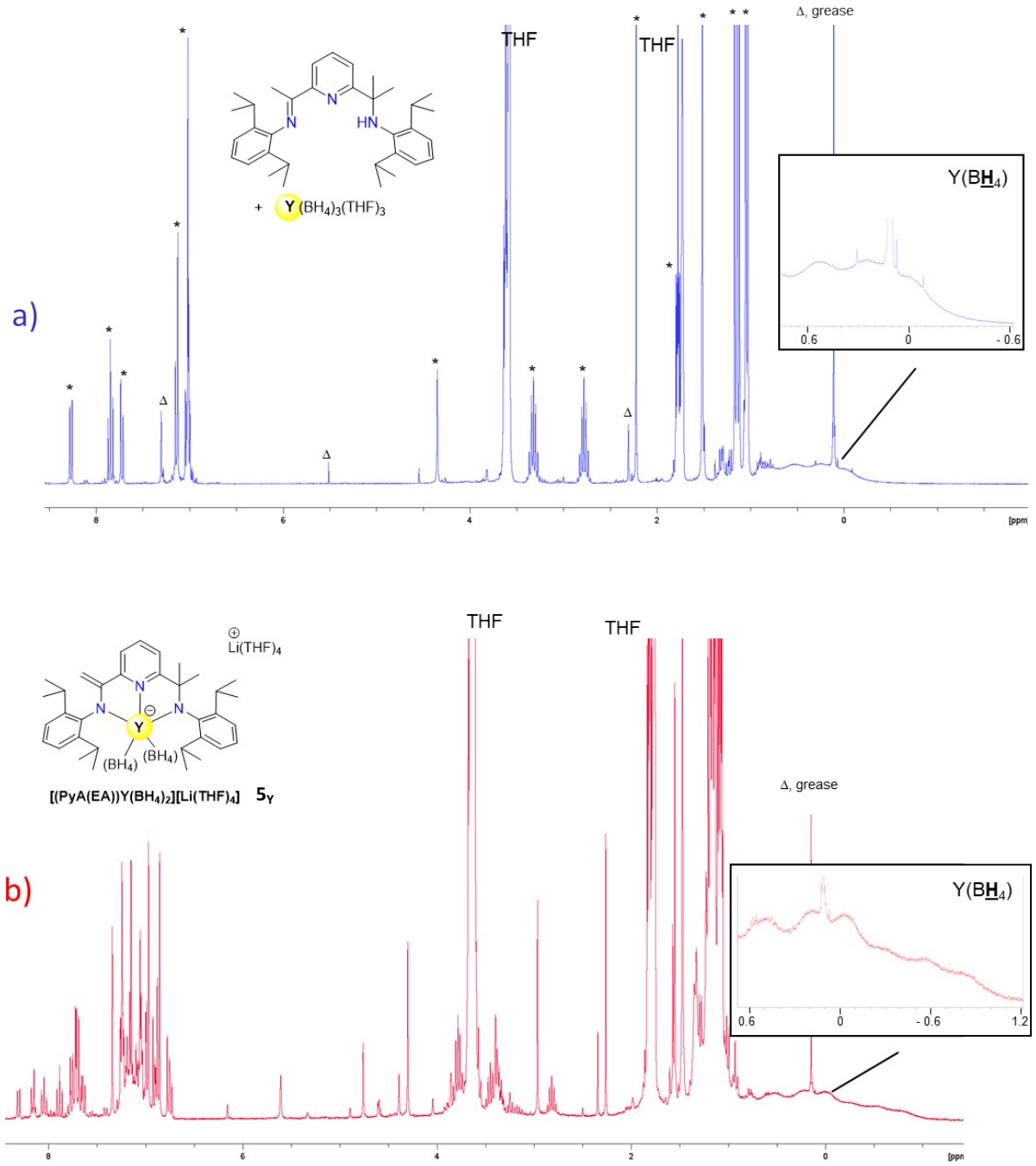

Fig. S11 ^{1}H NMR spectrum of the mixture $Y(BH_4)_3(THF)_3$ and 1 equiv. of **PyAH³** (a, top, blue, * **PyAH³** and Δ impurities) and of the isolated complex [(**PyA(EA)**)$Y(BH_4)_2$][$Li(THF)_4$] (**5$_Y$**)(b, bottom, red) (solvent THF-D_8)

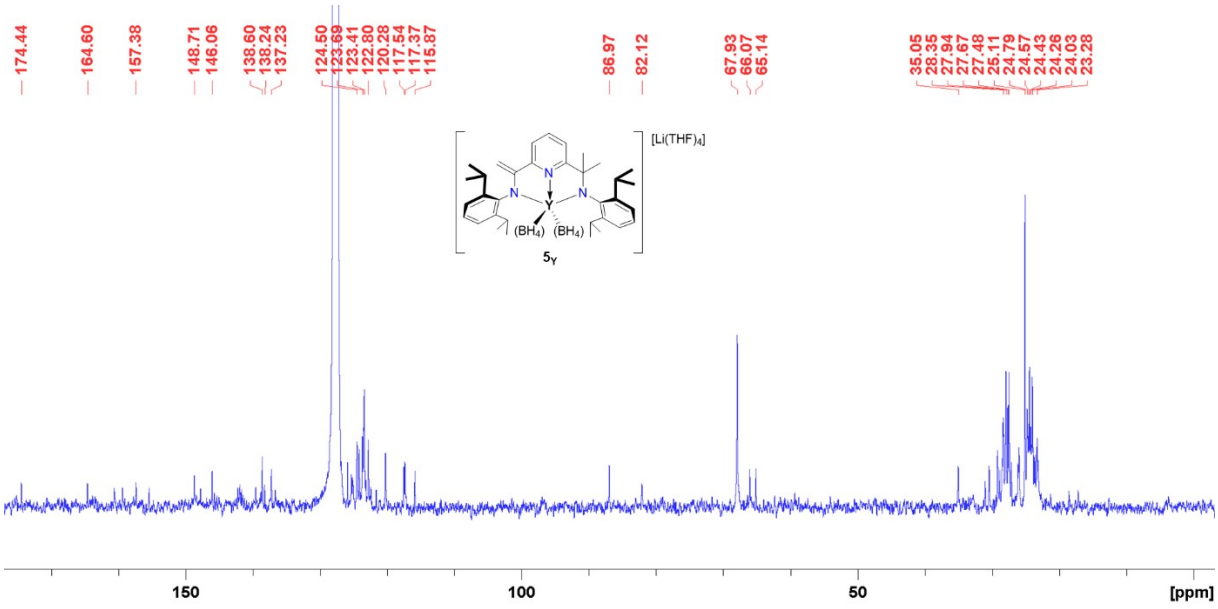

Fig. S12 ^{13}C NMR spectrum of **5$_Y$** in C_6D_6

^{13}C NMR (75 MHz, C_6D_6, Fig. S12): δ (ppm) = 23.28, 24.03, 24.26, 24.43, 24.57, 24.79, 25.11, 27.48, 27.67, 27.94, 28.35, 35.05, 65.14, 66.07, 67.93, 82.12, 86.97, 115.87, 117.37, 117.54, 120.28, 122.80, 123.41, 123.69, 124.50, 137.23, 138.24, 138.60, 146.06, 148.71, 157.38, 164.60, 174.44.

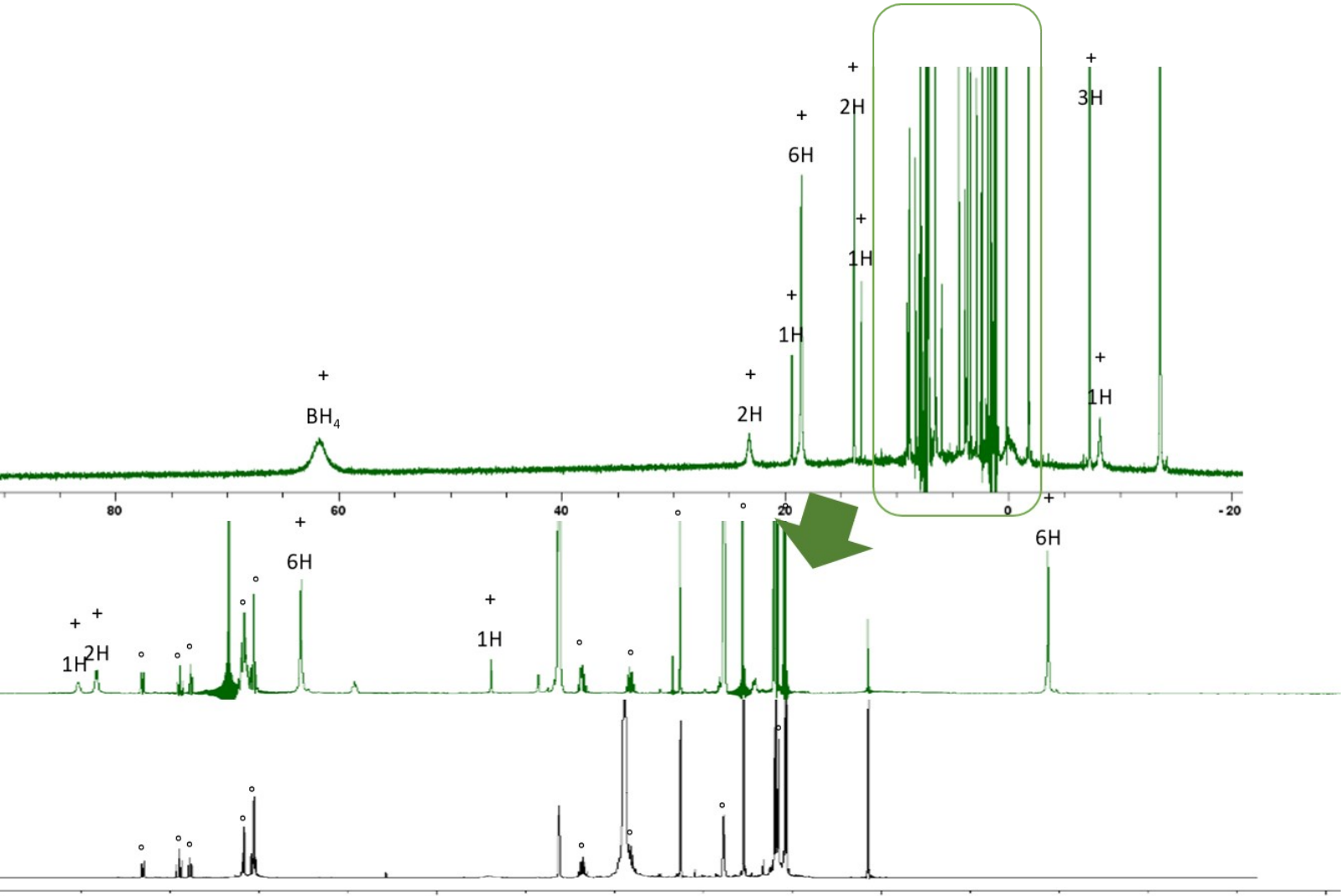
BH4
2H
6H
1H
2H
1H
3H
1H
80
60
40
20
0
-20
6H
6H
1H
1H
2H

Figure S13 ^{1}H NMR spectrum of paramagnetic complex (**PyA^{3}**)Nd(BH_4)$_2$ (**4$_{Nd}$**, green line) and comparison with ligand **PyAH^{3}** alone (black line, solvent THF-D_8)

Fig. S14 View of the molecular structure of (**PyA^{2}**)Mg(BH_4)(THF) (**3$_{Mg}$**) with ligand **PyA$^{2(S)}$**, hydrogen atoms have been omitted for more clarity apart from H7. Thermal ellipsoids are drawn at the 30% probability level. Selected distances (Å) and torsion angles (°): Mg-B1 = 2.2685(12), Mg-N1 = 2.1261(8), Mg-N2 = 1.9631(8), N1-C6-C7-N2 = -10.89(11), Pyr *vs.* N(amido)-aryl plan = 72.08(3).

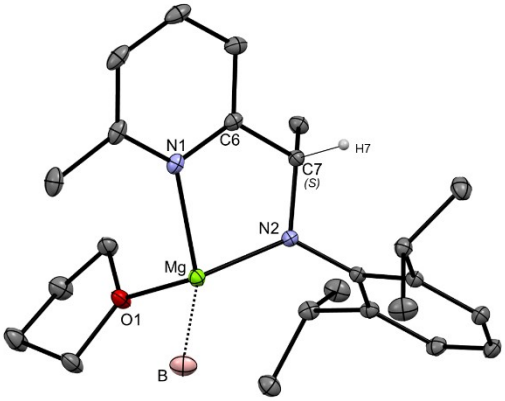

The magnesium complex **3$_{Mg}$** crystallized in the $P2_1/c$ space group. The unit cell for that complex contains two similar molecules with the two enantiomeric (*R*) and (*S*) ligands coordinated to the metal center (Fig. SX). The fourth-coordinated Mg center adopts a distorted tetrahedral geometry. The molecular structure displays shorter N(amido)-Mg [Mg-N2 = 1.9631(8) Å] and N(Pyr)-Mg [Mg-N1 = 2.1261(8) Å] bond lengths than in the yttrium complex **1$_{Y}$** [Y-N(Pyr) = 2.460(2) Å and Y-N(amido) = 2.205(2) Å], in accordance with the ligand being closer to the metal center in **3$_{Mg}$** than in **1$_{Y}$**. The Mg-B bond distance of 2.2685(12) Å is in a typical range for a η^3 coordination mode to magnesium. In this structure, the amido-pyridine chelate is slightly distorted as seen with the torsion angle N1-C6-C7-N2 of -10.89(11)°, while the N-aryl plane and the pyridine ring are not orthogonal to each other, with an angle of 72.08(3)° between them.

Fig. S15 Molecular structure of (**PyA^3**)Mg(BH_4)(THF) (**4$_{Mg}$**), with the hydrogen atoms omitted for clarity. Thermal ellipsoids are drawn at the 30% probability level. Selected distances (Å) and torsion angles (°): Mg-B1 = 2.328(2), Mg-N1 = 2.0587(16), Mg-N2 = 2.1507(16), Mg-N3 = 2.4081(16), N1-C13-C16-N2 = -0.4(2), N2-C20-C21-N3 = 1.7(2), Pyr *vs.* N(amido)-aryl plan = 95.32(3), Pyr *vs.* N(imine)-aryl plan) = 97.37(7).

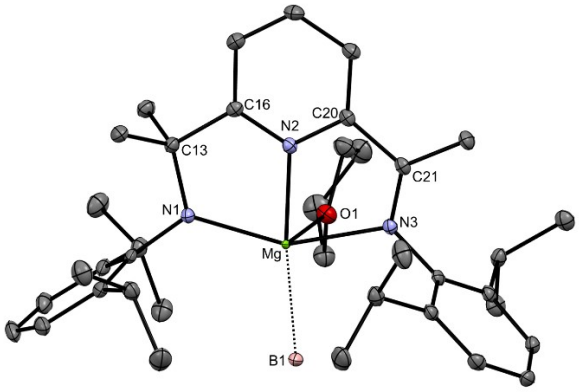

Like magnesium complex **3$_{Mg}$**, **4$_{Mg}$** crystallized in the $P2_1/c$ space group. The molecular structure of **4$_{Mg}$** (Fig. SX) displays a neutral magnesium center supported by the tridentate **PyA^3** ligand and a borohydride group, which is completed by an additional THF molecule. The Mg center adopts a distorted octahedral geometry, with the three nitrogen-magnesium bond distances unequal. Notably, the N(imino)-Mg bond stands out as the longest [N3-Mg = 2.4081(16) Å], whereas the N(amido)-Mg bond emerges as the shortest [N2-Mg = 2.0587(16) Å]. The latter is still longer than its counterpart in **3$_{Mg}$**, possibly due to the additional coordination of the imino arm in **4$_{Mg}$**. Meanwhile, the N(Pyr)-Mg bond length [N1-Mg = 2.1507(16) Å] remains consistent with that observed in **3$_{Mg}$**. Furthermore, the carbon-imine bond length [C21-N3 = 1.284(2) Å] falls within the typical range for C(sp2)-N bond distances. As same as with **3$_{Mg}$**, the magnesium borohydride distance of 2.328(2) Å in **4$_{Mg}$** is consistent with a BH_4-coordination in tri-hapto mode. Both N-aryl planes and pyridine ring are practically orthogonal with an angle of 97.37(7)° for the plane made by the N-aryl imine moiety and 95.32(6)° for the plane of the N-aryl amido part, while both amido and imino-pyridine chelates are almost coplanar, as demonstrated by the twist angle values [N1-20-C21-N3 = 1.7(2)°, N1-C16-C13-N2 = -0.4(2)°]. The orthogonality of the N-aryl plane along with the planarity of the amido/imino-pyridine moieties versus the pyridine ring are more marked for this magnesium complex **4$_{Mg}$** than for **3$_{Mg}$**. Finally, a quick comparison of Mg complexes allows to note that the Mg–N (pyridine and amido) and Mg–B present in both magnesium complexes (**3$_{Mg}$** and **4$_{Mg}$**) are in the same distances range. Probably caused by the rigidity induced by the imine moiety, the amido-pyridine chelate observed in **4$_{Mg}$** is more planar than that observed in complex **3$_{Mg}$** where **PyA^2** is coordinated.

Figure S16 SEC traces of isolated PLAs from Table 4

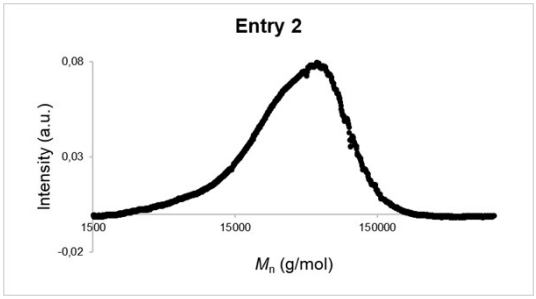

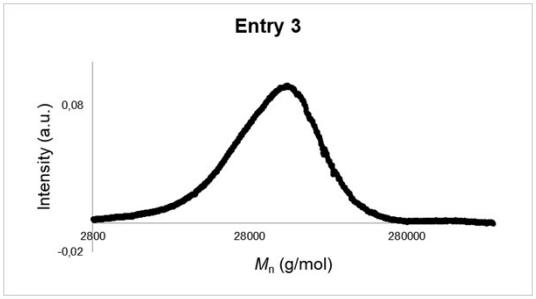

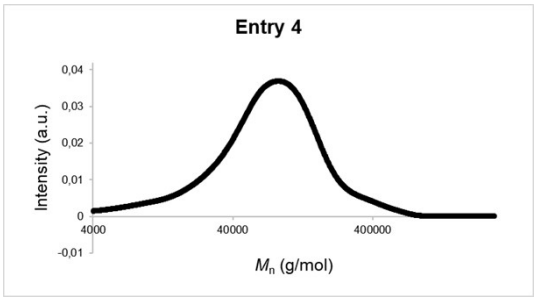

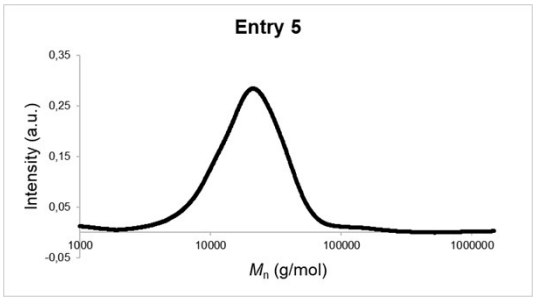

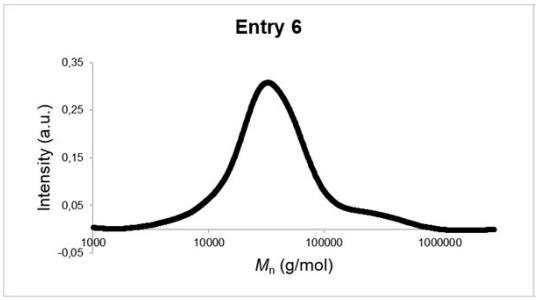

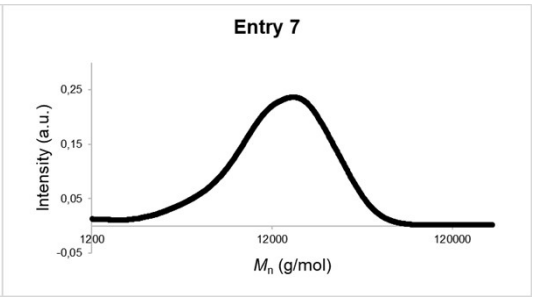

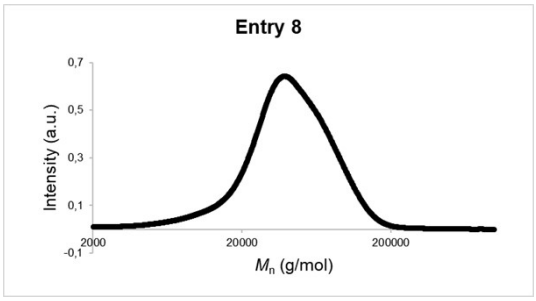

Figure S17 SEC traces of isolated PCLs from Table 5

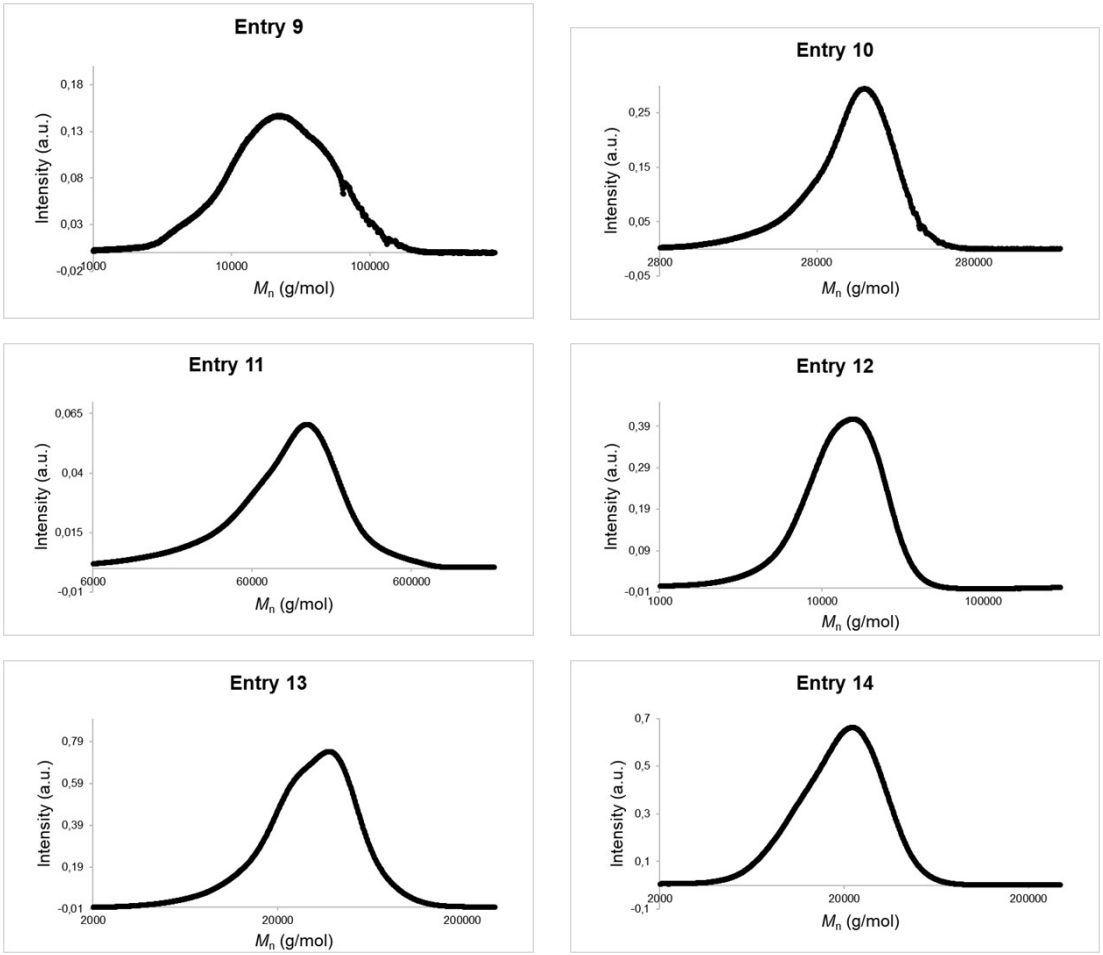

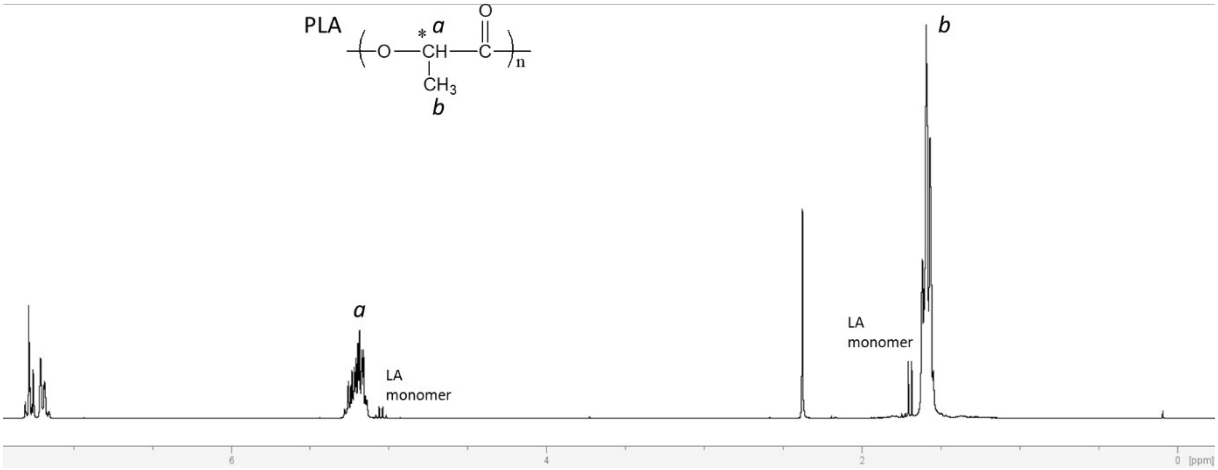

Figure S18 ^{1}H NMR of crude PLA issued from Entry 8 ($CDCl_3$)

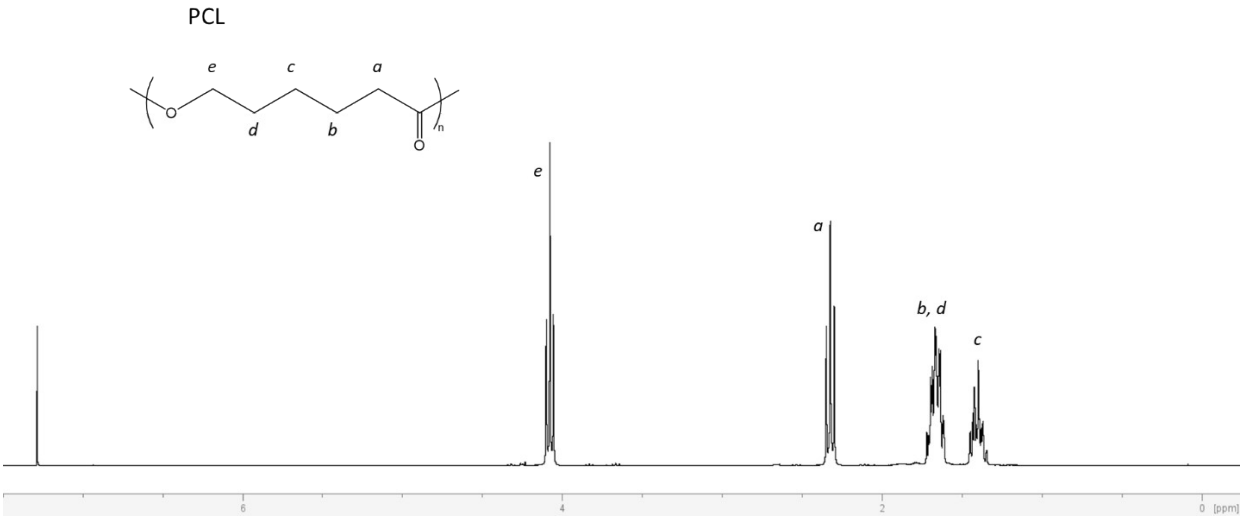

Figure S19 ^{1}H NMR of PCL isolated from Entry 11 ($CDCl_3$)

References

[1] A. W. Addison, T. N. Rao, J. Reedijk, J. van Rijn and G. C. Verschoor, Synthesis, structure, and spectroscopic properties of copper(II) compounds containing nitrogen–sulphur donor ligands; the crystal and molecular structure of aqua[1,7-bis(N-methylbenzimidazol-2'-yl)-2,6-dithiaheptane]copper(II) perchlorate, *J. Chem. Soc., Dalton Trans*., 1984, **7**, 1349. The calculation of this τ parameter in a five substituents system such as this one allows us to determinate the constraint on the metal and the percentage of distortion from a square pyramidal to a trigonal bipyramidal geometry. The value of τ oscillates between 0 and 1 where 0 correspond to a perfect square pyramidal geometry and 1 to a trigonal bipyramidal geometry. This geometric parameter was determined by the equation: $\tau = (\beta-\alpha)/60$ where β is the largest angle of the base (here N1-Y-B1 = 155.9°) and α is the second largest angle (here N2-Y-B2: 128.2°).